Acta Pharmacologica Sinica

www.nature.com/aps

ARTICLE

TIGAR knockdown enhanced the anticancer effect of aescin via regulating autophagy and apoptosis in colorectal cancer cells

Bin Li[1,2,3], Zhong Wang[4], Jia-ming Xie[4], Gang Wang[2], Li-qiang Qian[2], Xue-mei Guan[2], Xue-ping Shen[2], Zheng-hong Qin[3], Gen-hai Shen[2], Xiao-qiang Li[1] and Quan-gen Gao[2]

Our previous study showed that TP53-induced glycolysis and apoptosis regulator (TIGAR) regulated ROS, autophagy, and apoptosis in response to hypoxia and chemotherapeutic drugs. Aescin, a triterpene saponin, exerts anticancer effects and increases ROS levels. The ROS is a key upstream signaling to activate autophagy. Whether there is a crosstalk between TIGAR and aescin in regulating ROS, autophagy, and apoptosis is unknown. In this study, we found that aescin inhibited cell viability and colony formation, and induced DNA damage, cell cycle arrest, and apoptosis in cancer cell lines HCT-116 and HCT-8 cells. Concurrently, aescin increased the expression of TIGAR, ROS levels, and autophagy activation. Knockdown of TIGAR enhanced the anticancer effects of aescin in vitro and in vivo, whereas overexpression of TIGAR or replenishing TIGAR downstream products, NADPH and ribose, attenuated aescin-induced apoptosis. Furthermore, aescin-induced ROS elevation and autophagy activation were further strengthened by TIGAR knockdown in HCT-116 cells. However, autophagy inhibition by knockdown of autophagy-related gene *ATG5* or 3-methyladenine (3-MA) exaggerated aescin-induced apoptosis when TIGAR was knocked down. In conclusion, TIGAR plays a dual role in determining cancer cell fate via inhibiting both apoptosis and autophagy in response to aescin, which indicated that inhibition of TIGAR and/or autophagy may be a junctional therapeutic target in treatment of cancers with aescin.

Keywords: TIGAR; aescin; apoptosis; autophagy; colorectal cancer

Acta Pharmacologica Sinica (2019) 40:111–121; https://doi.org/10.1038/s41401-018-0001-2

INTRODUCTION

Colorectal cancer (CRC), the third most commonly diagnosed cancer in the world [1] is a major contributor to cancer morbidity and mortality [2, 3]. As multidrug resistance (MDR) is one of the significant attributions to result in the insensitivity of chemotherapy, recurrence and distant metastasis are the major causes of death [4]. Over the past several decades, many investigations have disclosed that several critical genes and aberrant molecular signaling pathways, including WNT/APC/β-catenin, EGFR, RAS/MAPK, PI3K/AKT/GSK3β, TGF-β, NF-κB, TP53, and DNA mismatch-repair pathways, are important for the initiation and progression of CRC [5, 6].

TP53-induced glycolysis and apoptosis regulator (TIGAR), a p53-inducible protein, functions to decrease fructose-2,6-bisphosphate (Fru-2,6-P2) levels in cells, and retunes cell metabolism from glycolysis to pentose phosphate pathway (PPP), resulting in increases in ribose and NADPH, the latter reduces oxidized glutathione (GSSG) to GSH and decreases reactive oxygen species (ROS) [7]. TIGAR lowers intracellular ROS and suppresses autophagy in response to nutrient starvation or metabolic stress, and functions to inhibit apoptosis [8]. TIGAR, as an oncogene protein, is overexpressed in breast cancer [9], glioblastomas [10], cytogenetically normal (CN-) AML patients [11], nasopharyngeal carcinoma [12], and CRC [13]. Of note, TIGAR plays a key role in intestinal proliferation and tumor initiation. In TIGAR-deficient mice, deficiency of TIGAR, NADPH, and nucleosides reduced small intestine proliferation and regeneration capacity in response to acute damage, and also reduced the tumor burden in intestinal adenoma model, which indicates that TIGAR and its downstream products of NADPH and nucleosides are required for the development of intestinal adenoma [14]. More importantly, our previous results demonstrated that TIGAR had a dual function in regulation of autophagy and apoptosis in epirubicin-treated cells [15]. Furthermore, we also found that TIGAR relocalizes to nucleus after epirubicin- or hypoxia-treated cancer cells and rescues cells from apoptosis via regulating CDK5/ATM pathway to reduce DNA damage and promote DNA repair [16].

Aescin, a triterpene saponin separated from horse chestnut seed, was demonstrated to have anticancer effects over the past decades. Aescin induces growth arrest at the G1-S phase in CRC

[1]Department of Vascular Surgery, The Second Affiliated Hospital of Soochow University, Suzhou 215007, China; [2]Department of General Surgery, The First People's Hospital of Wu Jiang, Suzhou 215200, China; [3]Department of Pharmacology and Laboratory of Aging and Nervous Diseases, Jiangsu Key Laboratory of Translational Research and Therapy for Neuro-Psycho-Diseases, Jiangsu Key Laboratory of Preventive and Translational Medicine for Geriatric Diseases, College of Pharmaceutical Science, Soochow University, Suzhou 215123, China and [4]Department of General Surgery, The Second Affiliated Hospital of Soochow University, Suzhou 215007, China
Correspondence: Gen-hai Shen (wjsgh3026@sina.com) or Xiao-qiang Li (flytsg@126.com) or Quan-gen Gao (wjyygqg@sohu.com)
These authors contributed equally: Bin Li, Zhong Wang and Jia-ming Xie.

Received: 8 October 2017 Accepted: 15 January 2018
Published online: 16 May 2018

cells and inhibits the formation of colonic aberrant crypt foci (ACF) in rats [17]. Aescin suppresses cell proliferation and survival via inhibiting the activation of signal transducer and activator of transcription 3/Janus-activated kinase 2 (STAT3/JAK2) [18, 19] and NF-κB pathway, as well as synergistically potentiates the anticancer effect of other chemotherapeutic drugs [20]. Specifically, aescin synergistically potentiates the chemotherapeutic effect of 5-FU in HCC [21] and gemcitabine in pancreatic cancer cell [22]. Moreover, aescin also reverses MDR [23] and suppresses migration and invasion in different cancer cells [24, 25].

TIGAR promotes tumor development via metabolic regulation and DNA repair. More importantly, TIGAR regulates autophagy and apoptosis in response to stress and cancer therapy. Aescin increases the levels of cellular ROS [26] that are key upstream signaling to activate autophagy [27]. However, whether TIGAR regulating autophagy and apoptosis determines cancer cell fate in response to aescin is unclear. In the present study, we focused on the functions of TIGAR in regulating DNA damage, ROS, autophagy, and apoptosis, by which TIGAR affected the anticancer effects of aescin. TIGAR partly protected cancer cells from apoptosis via decreasing DNA damage, promoting DNA repair, scavenging ROS, and regulating autophagy. Moreover, inhibition of autophagy increased aescin-induced apoptosis when TIGAR was knocked down. These data provided evidence that TIGAR and autophagy may be a potential therapeutic target in treatment of CRC with aescin.

MATERIALS AND METHODS

Materials and regents

Aescin was supplied by Shandong Luye Pharmaceutical Co., Ltd. (Yantai, China), dissolved in normal saline (NS), and diluted just before using. 3-MA was purchased from Sigma-Aldrich (St Louis, MO, USA). Hoechst 33342 was purchased from Beyotime (Shanghai, China). Epirubicin (Epi) was purchased from the First People's Hospital of Wujiang (Suzhou, China).

Cell culture

Human colorectal cancer HCT-116 and HCT-8 cells were obtained from the Chinese Academy of Sciences (Shanghai, China) and human normal colon NCM460 cells were kept in the laboratory of College of Pharmaceutical Science (Suzhou, China). Cells were cultured with Dulbecco's Modified Eagle Medium (DMEM; GIBCO, C11965500BT) containing 10% fetal bovine serum (FBS; GIBCO; 10270-106), 100 IU/mL penicillin, and 100 IU/mL streptomycin in a humidified incubator at 37 °C under 5% CO_2 atmosphere.

Cell counting kit-8 (CCK-8) analysis and colony formation analysis

Cells were seeded in 96-well plates (3000 cells/well). After a series of treatment, cells were added 10 μL of CCK-8 (CK04-3000T, Dojindo, Japan) and incubated at 37 °C for 2–4 h. The absorbance was measured at 450 nm with a microculture plate reader (Bie Tek). The percentage of growth inhibition was estimated by the absorbance.

As for colony formation assay, HCT-116 and HCT-8 cells were cultured in 6-well plates (200 cells/well) for 36 h, and then were treated with different concentrations of aescin (0, 5, 10, and 20 μg/mL) for 12 or 14 days until clones were visible. The medium was discarded and the clones were stained with crystal violet (C0121, Beyotime, Shanghai, China) for 15 min at room temperature. After washed six times with double distilled water, the clones were counted and photographed.

RNA interference and genes overexpression

To inhibit autophagy, *ATG5* siRNAs (GCAACUCUGGAUGGGAUUGTT, *ATG5* siRNA1; CAUCUGAGCUACCCGGAUATT, *ATG5* siRNA2) were synthesized by GenePharma (Shanghai, China), and a scramble sequence (UUCUCCGAACGUGUCACGUTT) was synthesized as a negative control. To inhibit the expression of TIGAR, two siRNAs (GCAGCAGCTGCTGGTATAT; *TIGAR* siRNA1; TTAGCAGCCAGTGTCTTAG; *TIGAR* siRNA2) were synthesized by GenePharma, and a scramble sequence (TTACCGAGACCGTACGTAT) was synthesized as a negative control [15]. To overexpress TIGAR, the TIGAR plasmid (Flag-TIGAR) was transfected. Lipofectamine™ RNAiMAX and Lipofectamine 3000 (Invitrogen, USA) were used and the procedures were conducted as previously described [15].

Western blotting analysis (WB)

Preparation of total protein lysates and western blotting analysis was performed as described previously [15, 28]. The primary antibodies against PARP (#9532), γ-H2AX (#9718), p53 (#2524), ATG5-ATG12 (#12994), cleaved-caspase-9 (#9505), and cleaved-caspase-3 (#9661 and 9664) were from Cell Signaling Technology (CST, Danfoss, MA, USA). Cleaved-caspase-3 was also from ENZO Life Sciences (Lot No. 11021102 Farmingdale, NY, USA). β-Actin (A5441) and p62 (P0067) were from Sigma-Aldrich (St Louis, MO, USA). LC3 was from MBL (M186-3, Nagoya, Japan), TIGAR were from Abcam (#37910, Cambridge, UK). Fluorescence secondary antibodies (1:10,000; Jackson ImmunoResearch, anti-rabbit, 711-035-152, anti-mouse, 715-035-150) were used. Immunoreactivity was detected using Odyssey Infrared Imager (Li-COR Biosciences).

HCT-116 cells xenograft mice models

HCT-116 cells were infected with lentivirus of EGFP-LV-shRNA-TIGAR (TIGAR: 5′-GATTAGCAGCCAGTGTCTTAG-3′; Shanghai Genechem Co., Ltd., Shanghai, China) to inhibit the expression of TIGAR. The lentivirus of EGFP-LV-shRNA-NC was used as negative control. The level of TIGAR was successfully decreased. The infected cells (2×10^6) were subcutaneously inoculated into the right iliac fossa of 6-week-old female athymic nude mice (Shanghai SLAC Laboratory Animal Co. Ltd.). The body weight of mice was measured weekly and the tumor growth was measured twice weekly using a caliper. The tumor volume was calculated as: volume (mm^3) = (length × width^2) × Π/6. When the tumors grew to the volume of 150–200 mm^3, aescin (2 mg/kg) was intraperitoneally injected into mice every day for 12 days. Tumor sizes were measured every 3 days when aescin was treated. The mice were killed, and the tumors were removed and photographed. The weight of tumors was measured. Tumor proteins were extracted for western blotting analysis. Tumor tissues were also used for immunohistochemistry. All animal procedures were approved and monitored by the local Animal Care and Use Committee in Soochow University.

Flow cytometry (FCM) detection of apoptosis, cell cycle, and ROS

The detection of apoptosis by flow cytometry (FCM) was performed as described previously [15]. In briefly, after a series of treatment, freshly trypsinized cells were collected, washed twice with PBS, and processed following the manufacturer's instructions. Cell apoptosis, cell cycle, and ROS were quantified with double staining of Annexin V-FITC and propidium iodide (PI) (Biouniquer, BU-AP0103), PI and H2-DCFDA (Beyotime, Shanghai, China), respectively. Ten thousands cells per sample were acquired with a FCMcan flow cytometer (FCMcan). Cell fluorescence was analyzed with flow cytometry using the Cell Quest Pro software (Beckman Coulter).

Immunohistochemistry (IHC)

The paraffin-embedded sections (5 μm thick) were prepared for examining the expressions of TIGAR, γ-H2AX, and Ki-67 (mouse anti-Ki-67: GeneTex Inc., Irvine, CA, USA) by immunohistochemistry with the streptavidin-peroxidase (S-P) kit (Fuzhou Maixin Biotechnology Development Co., Fuzhou, China). The detail procedures were performed as described previously [29].

Hoechst staining
The effects of aescin on DNA damage and apoptosis were evaluated using Hoechst 33342 staining. Cells were treated with 0, 20, 40, and 60 μg/mL aescin for 12 h. Then, cells were fixed in 4% paraformaldehyde and stained with Hoechst 33342 (10 μg/mL). Apoptotic nuclei were analyzed with laser scanning confocal microscopy (Nikon, C1S1, Tokyo, Japan).

Statistical analysis
Data were subjected to one-way ANOVA using the GraphPad Prism 6 software statistical package (GraphPad Software, Inc., La Jolla, CA, USA). When a significant group effect was found, post hoc comparison were performed using the Newman–Keuls *t* test to examine special group differences. $^{*}P < 0.05$, $^{**}P < 0.01$, $^{***}P < 0.001$, and $^{****}P < 0.0001$ are considered to be significant. ns, $P > 0.05$ vs. corresponding group.

RESULTS

Aescin inhibited the proliferation of CRC cells
To explore the inhibitory effects of aescin on cell proliferation and viability, colorectal cancer HCT-116 and HCT-8 cells were treated with various concentrations of aescin for 12, 24, and 48 h. Cell viability was evaluated with CCK-8 assay. As shown in Fig. 1a, b, aescin significantly reduced the cell viability of HCT-116 and HCT-8 cells in a dose- and time-dependent manner. The IC_{50} values of aescin were 84.64 ± 4.57, 60.12 ± 5.31, and 36.70 ± 2.15 μg/mL for 12, 24, and 48 h in HCT-116 cells, as well as 107.05 ± 14.22, 83.55 ± 6.99, and 46.99 ± 2.81 μg/mL for 12, 24, and 48 h in HCT-8 cells, respectively. In addition, we detected the inhibitory effects of aescin in normal colon NCM460 cells. As shown in Fig. 1c, the IC_{50} values of aescin in NCM460 cells were 123.0 ± 0.70, 117.1 ± 0.21, and 89.71 ± 0.15 μg/mL for 12, 24, and 48 h, respectively. Although aescin inhibited the cell viability of NCM460 cells, especially with treatment of 80 or 100 μg/mL aescin for 24 and 48 h, the cell viability was not significantly inhibited in NCM460 cells treated with 40 or 60 μg/mL aescin for 12 h. Therefore, treatment cells with 40 or 60 μg/mL aescin for 12 h were administrated to illustrate the mechanisms by which aescin regulated ROS, autophagy, and apoptosis in the following studies.

Moreover, the long-term inhibition on cell proliferation by aescin was detected with colony formation assay. Similarly, aescin clearly inhibited the colony formation of the two cell lines in a dose-dependent manner (Fig. 1d, e). These results indicated that aescin inhibited the proliferation of CRC cells.

Aescin-induced DNA damage, cell cycle arrest, and apoptosis of CRC cells
Previous studies illustrated that aescin increased cellular ROS levels [26], whereas, there is few evidence to determine whether aescin induces DNA damage. In order to determine the DNA damage induced by aescin, PARP and γ-H2AX, two DNA damage-associated markers, were detected with western blotting. As shown in Fig. 2a, b, aescin significantly increased the levels of activated PARP and γ-H2AX in a dose- and time-dependent manner. As a positive control, epirubicin (Epi) also produced DNA damage in HCT-8 cells. Next, we detected whether aescin induced cell cycle arrest. As shown in Fig. 2c, d, aescin significantly induced G1 phase arrest in a dose-dependent manner. The efficiency of G1 phase arrest in response to aescin was 49.37%, 54.33%, 60.14%, and 68.51% in HCT-116 cells treated with 0, 20, 40, and 60 μg/mL aescin for 12 h, as well as 59.58%, 63.76%, 68.5%, and 73.99% in HCT-8 cells, respectively.

Furthermore, Hoechst staining was performed to explore the chromatin condensation and fragmentation in response to aescin. High concentrations of aescin (40 and 60 μg/mL) significantly induced chromatin condensation and fragmentation in HCT-116 and HCT-8 cells (Fig. 2e, f). Severe DNA damage may lead to cell apoptosis [30]. To further explore whether aescin-induced DNA damage could potentiate aescin-induced apoptosis, cell apoptosis was measured by Annexin V-FITC/PI staining and FCM method. After treatment with aescin (20, 40, 60, and 80 μg/mL) for 12 h, the apoptotic percentages were 12.81 ± 2.38%, 30.12 ± 3.21%, 45.32 ± 3.21%, and 77.86 ± 7.65% in HCT-116 cells, and 6.25 ± 1.27%, 23.86 ± 1.41%, 39.78 ± 3.14%, and 60.55 ± 6.16% in HCT-8 cells, respectively (Fig. 2g, h). These results showed that aescin could induce DNA damage and apoptosis in HCT-116 and HCT-8 cells.

Aescin-induced TIGAR upregulation and knockdown of TIGAR deteriorated aescin-induced apoptosis of CRC cells
Our previous results demonstrate that TIGAR regulates DNA damage and apoptosis in response to chemotherapeutic drugs [15, 16]. Next, we further investigated whether aescin regulates the expression of TIGAR and whether TIGAR is implicated in aescin-induced DNA damage and apoptosis. As shown in Fig. 3a, b, the levels of TIGAR were significantly elevated with treatment of 10, 20, and 40 μg/mL aescin for 12 h or treatment of 60 μg/mL aescin for 9, 12, and 24 h in HCT-116 and HCT-8 cells. Previous evidence has shown that TIGAR is a downstream protein of TP53; [7] however, there is still a TP53-independent pathway to induce the expression of TIGAR [31]. In this study, we found that the level of p53 was not increased in aescin-treated cancer cells, indicating that the elevation of TIGAR was independent of p53 in response to aescin (Fig. 3a, b).

To determine the role of TIGAR in aescin-induced apoptosis, TIGAR knockdown was performed with *TIGAR* siRNAs. *TIGAR* siRNA1/2 could effectively downregulate the expression of TIGAR in HCT-116 cells (Fig. 3c). TIGAR knockdown apparently augmented aescin-induced apoptosis in comparison with aescin treatment alone in HCT-116 cells (Fig. 3d). Furthermore, western blotting results showed that the levels of activated PARP, activated caspase-9, activated caspase-3, and γ-H2AX were higher in combination with TIGAR knockdown and aescin than aescin treatment alone in HCT-116 and HCT-8 cells (Fig. 3e, f). These results demonstrated that aescin upregulated the expression of TIGAR; knockdown of TIGAR deteriorated aescin-induced apoptosis.

Overexpression of TIGAR and replenishment of NADPH and ribose-attenuated aescin-induced DNA damage and apoptosis
To investigate the protective function of TIGAR in response to aescin, we constructed the TIGAR overexpression plasmids, and the level of TIGAR was effectively elevated in HCT-116 cells (Fig. 4a). Of note, TIGAR overexpression significantly attenuated aescin-induced DNA damage and apoptosis, as western blotting results showed that the levels of activated PARP, activated caspase-9, activated caspase-3, and γ-H2AX were apparently decreased in cells with overexpressing TIGAR in response to aescin (Fig. 4b), suggesting the DNA protective and apoptosis suppressive functions of TIGAR in HCT-116 cells. In line with the western blotting results, FCM results also showed that the apoptosis was significantly decreased when cells were overexpressed TIGAR in response to aescin (Fig. 4c).

TIGAR retunes cancer cell metabolism from glycolysis to PPP to produce NADPH and ribose, which plays key roles in DNA damage and apoptosis [7, 16]. We next investigated whether replenishment of NADPH and ribose could rescue aescin-induced DNA damage and apoptosis when TIGAR was knocked down. As shown in Fig. 4d, e, replenishment of NADPH and ribose markedly decreased the levels of activated PARP, activated caspase-9, and γ-H2AX induced by TIGAR knockdown and aescin, suggesting that NADPH and ribose functioned as the same roles as TIGAR overexpression to partly rescue the DNA damage and apoptosis. Moreover, FCM results consolidated the WB results that

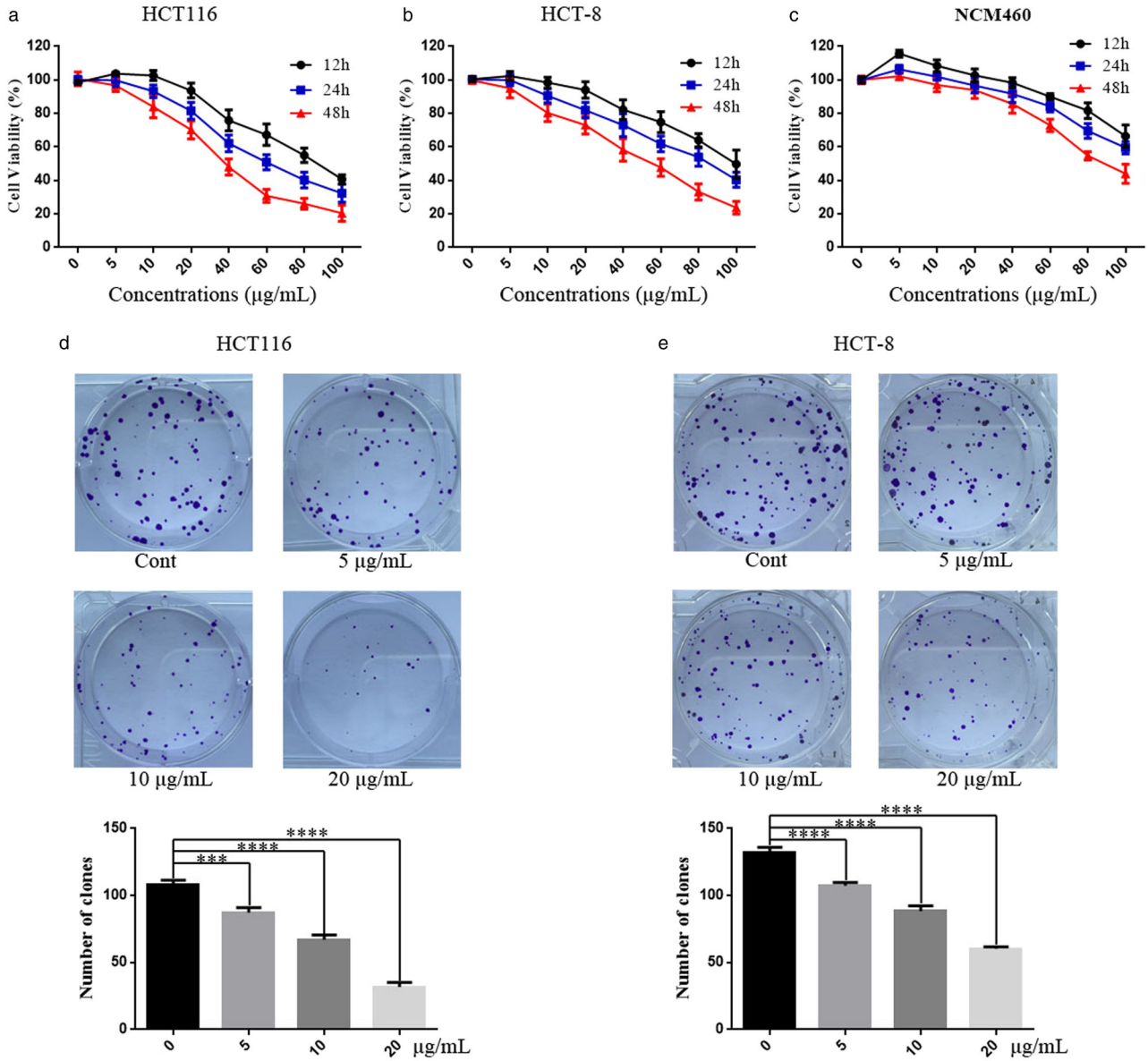

Fig. 1 Aescin inhibited the proliferation of CRC cells. **a**, **b**, **c** CCK-8 assay of cell viability in HCT-116, HCT-8, and NCM460 cells with treatment of 0, 5, 10, 20, 40, 60, 80, and 100 μg/mL aescin for 12, 24, and 48 h. **d**, **e** Colony formation assay of clones in HCT-116 and HCT-8 cells with treatment of 0, 5, 10, and 20 μg/mL aescin for 12 or 14 days. Quantitative analysis of the clone number in HCT-116 and HCT-8 cells. The values are means ± SD from three independent experiments. ***$P < 0.001$; ****$P < 0.0001$ vs. control group

replenishment of NADPH and ribose decreased aescin-induced apoptosis (Fig. 4f, g). These data demonstrated that TIGAR exerted a protective effect on aescin-induced DNA damage and apoptosis in CRC cells.

Knockdown of TIGAR enhanced the anticancer effect of aescin in vivo

To further evaluate the effect of TIGAR in vivo, HCT-116 cells were infected with the lentivirus of EGFP-LV-shRNA-TIGAR (MOI = 10) to downregulate the expression of TIGAR. The efficiency of lentiviral infection was determined with fluorescence in HCT-116 cells (Fig. 5a). The level of TIGAR was markedly decreased in infected LV-shRNA-TIGAR cells in comparison with the infected LV-shRNA-NC cells (Fig. 5b). A xenograft model was successfully established in nude mice using the infected HCT-116 cells, and the tumors were removed from mice (Fig. 5c). The body weight of mice was decreased with the administration of aescin in the first week; however, that was gradually increased in the second week, indicating that there were some toxic effects with treatment of aescin in vivo (Fig. 5d). More importantly, TIGAR knockdown and aescin apparently reduced the tumor volumes and weight in comparison with aescin treatment alone (Fig. 5e, f). Western blotting analysis of tumor tissue lysates revealed that the level of activated PARP was higher in combination with TIGAR knockdown and aescin than NC and aescin (Fig. 5g), which suggested that TIGAR knockdown increased aescin-induced apoptosis in vivo. Moreover, immunohistochemistry results showed that the level of γ-H2AX was increased in combination with TIGAR knockdown and aescin (Fig. 5h), indicating that TIGAR knockdown increased aescin-induced DNA damage in vivo. In addition, the level of TIGAR was apparently increased in aescin-treated NC group, while that was decreased in TIGAR knockdown groups (Fig. 5g, h). These results suggested that TIGAR knockdown enhanced the anticancer effect of aescin in vivo.

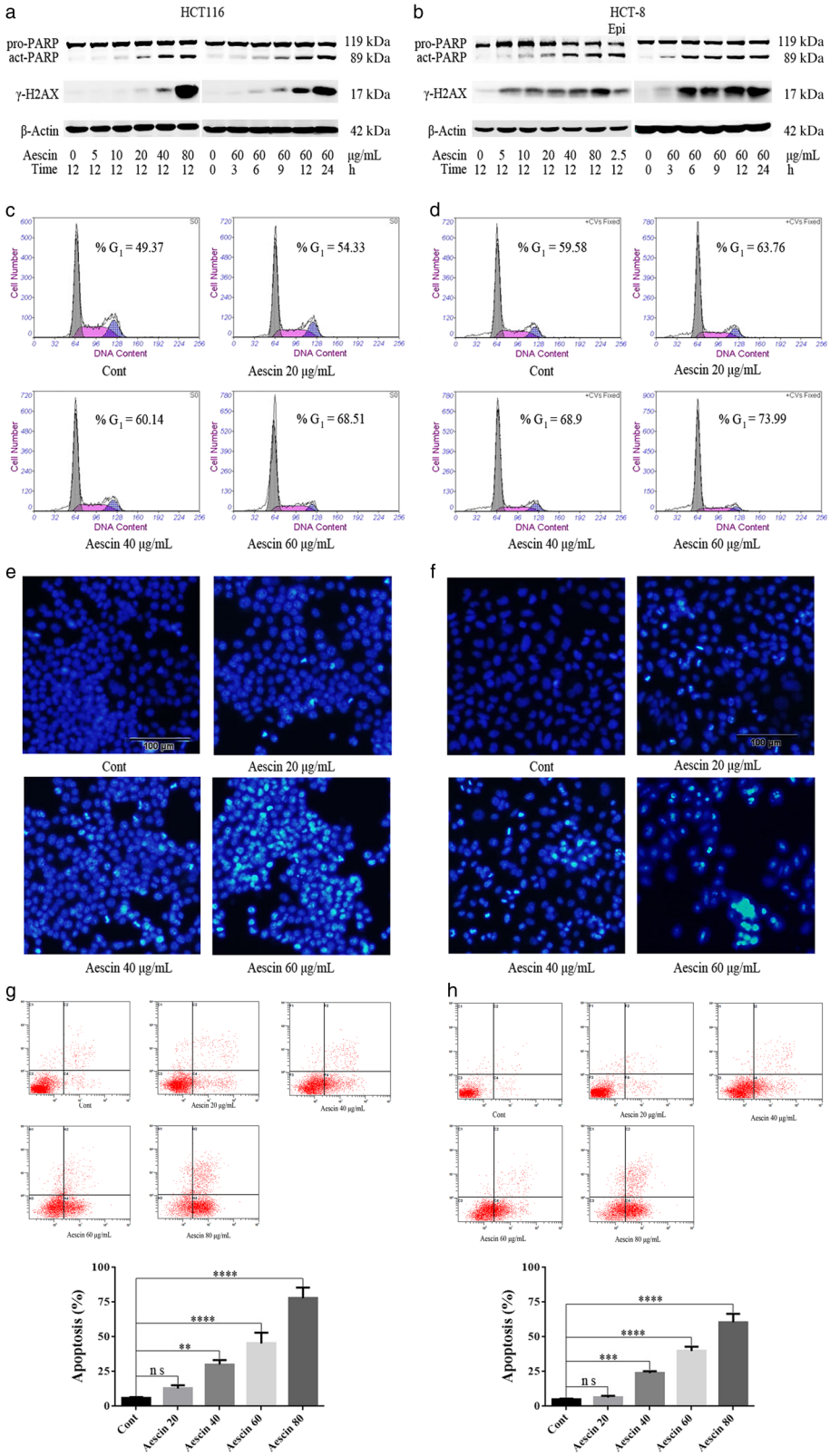

Fig. 2 Aescin induced DNA damage, cell cycle arrest, and apoptosis of CRC cells. **a**, **b** The levels of PRAP, γ-H2AX, and β-actin in HCT-116 and HCT-8 cells by western blotting analysis (WB). Cells were treated with 0, 5, 10, 20, 40, and 80 μg/mL aescin or 2.5 μg/mL epirubicin (positive control) for 12 h; and cells were treated with 60 μg/mL aescin for 0, 3, 6, 9, 12, and 24 h. β-actin was used as a loading control. **c**, **d** Flow cytometry (FCM) analysis of the cell cycle in HCT-116 and HCT-8 cells with treatment of 0, 20, 40, and 60 μg/mL aescin for 12 h. **e**, **f** Hoechst staining analysis DNA damage in HCT-116 and HCT-8 cells with treatment of 0, 20, 40, and 60 μg/mL aescin for 12 h. **g**, **h** FCM analysis of the apoptosis using double staining of Annexin V-FITC and PI in HCT-116 and HCT-8 cells with treatment of 0, 20, 40, 60, and 80 μg/mL aescin for 12 h. Quantitative analysis of aescin-induced apoptosis. The values are means ± SD from three independent experiments. $^{**}P < 0.01$; $^{***}P < 0.001$; $^{****}P < 0.0001$; $^{ns}P > 0.05$ vs. control group

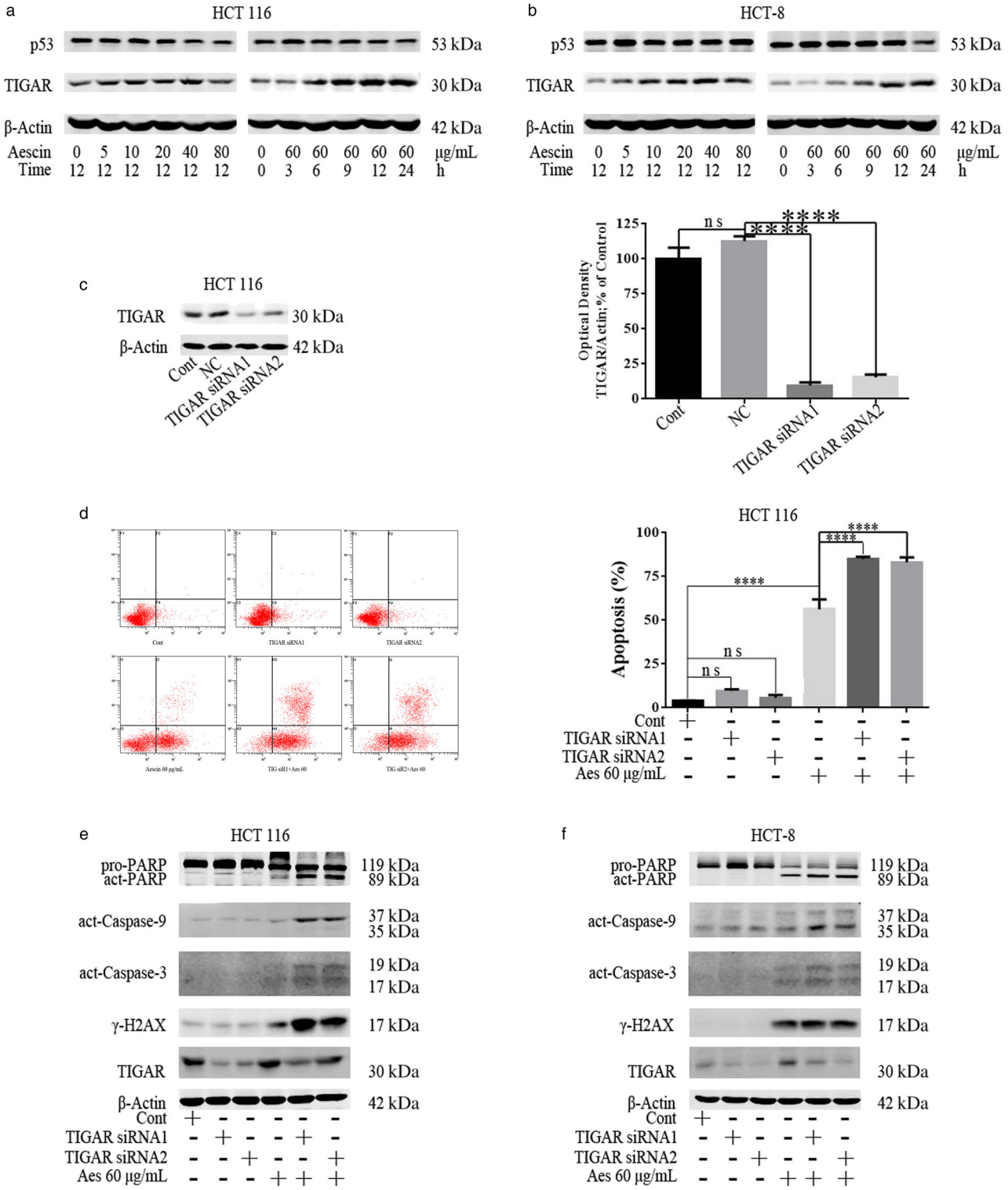

Fig. 3 Aescin-induced TIGAR upregulation and knockdown of TIGAR deteriorated aescin-induced apoptosis of CRC cells. **a**, **b** The levels of p53, TIGAR, and β-actin by WB. Cell treatment as described as Fig. 2a. **c** The levels of TIGAR and β-actin in HCT-116 cells by WB. Cells were transiently transfected with or without scramble siRNA, *TIGAR* siRNA1 and *TIGAR* siRNA2 for 48 h. Quantitative analysis of TIGAR knockdown efficiency in HCT-116 cells. **d** FCM analysis of the apoptosis in HCT-116 cells. Cells were treated with or without 60 μg/mL aescin for 12 h after cells were transfected with *TIGAR* siRNA1 or *TIGAR* siRNA2 for 36 h. Quantitative analysis of the apoptosis. **e**, **f** The levels of PRAP, activated caspase-9, activated caspase-3, γ-H2AX, TIGAR, and β-actin in HCT-116 and HCT-8 cells by WB. Cells were treated as **e** and **f**. β-actin was used as a loading control. The values are means ± SD from three independent experiments. ****$P < 0.0001$; $^{ns}P > 0.05$ vs. control group

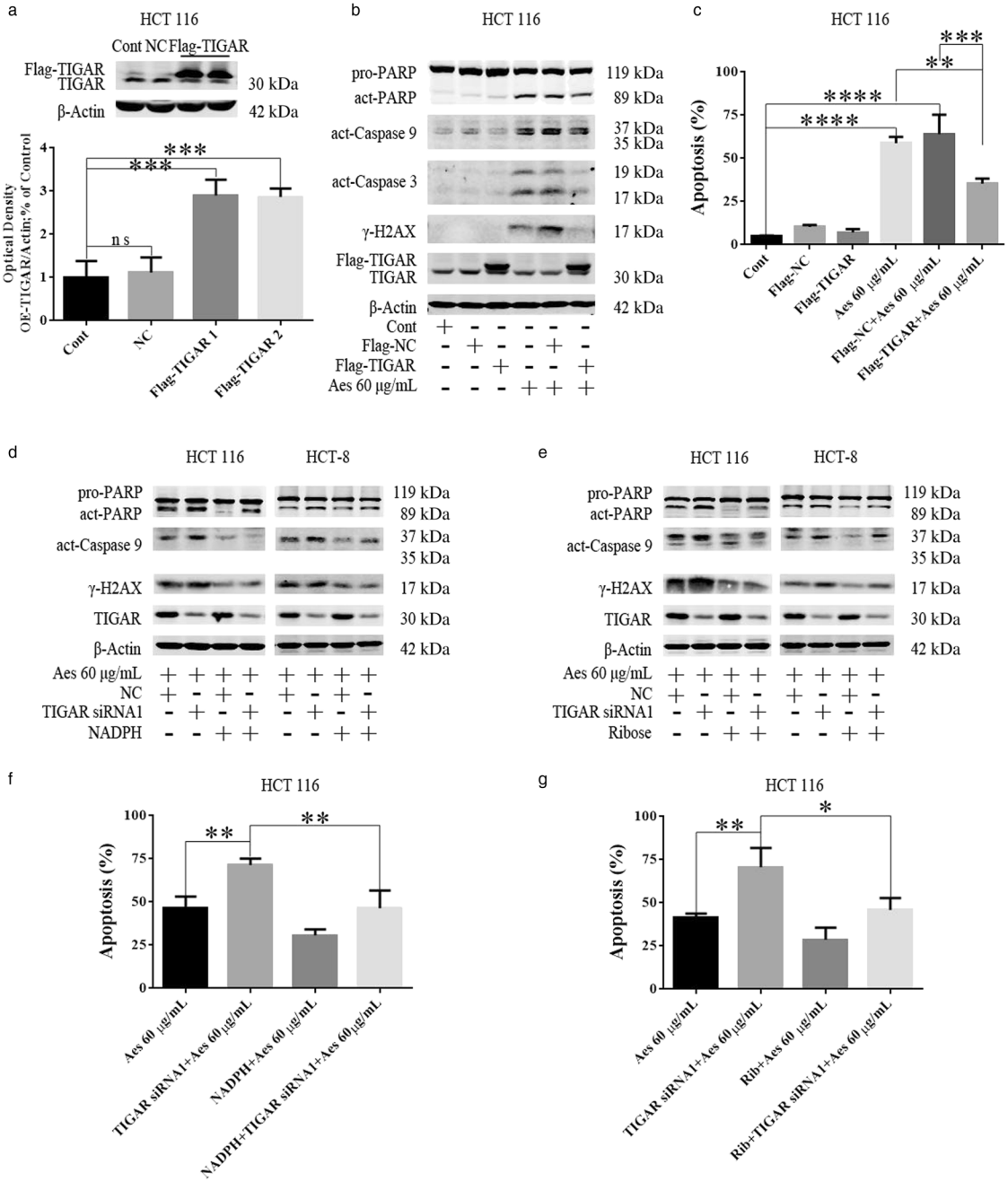

Fig. 4 Overexpression of TIGAR and replenishment of NADPH and ribose-attenuated aescin-induced DNA damage and apoptosis. **a** The levels of TIGAR and β-actin in HCT-116 cells by WB. Cells were transfected with or without Flag-NC and Flag-TIGAR plasmids for 36 h. Quantitative analysis of TIGAR overexpression efficiency in HCT-116 cells. **b**, **c** Cells were treated with or without 60 μg/mL aescin for 12 h after Flag-NC or Flag-TIGAR plasmid was transfected for 36 h. The levels of PRAP, activated caspase-9, activated caspase-3, γ-H2AX, TIGAR, and β-actin in HCT-116 cells by WB (B). FCM analysis of the apoptosis in HCT-116 cells (**c**). **d**, **e** The levels of PRAP, activated caspase-9, γ-H2AX, TIGAR, and β-actin in HCT-116 and HCT-8 cells by WB. Cells were transiently transfected with NC or TIGAR siRNA1 for 36 h, then cells were treated with 60 μg/mL aescin for 12 h. Before harvest, cells were treated with NADPH (**d**) or ribose (**e**) for 14 h. **f**, **g** FCM analysis of the apoptosis in HCT-116 cells. Cells were treated as described in **d** and **e**. β-actin was used as a loading control. The values are means ± SD from three independent experiments. $^{***}P < 0.001$; $^{ns}P > 0.05$ vs. control group

Aescin-activated autophagy and inhibition of autophagy and TIGAR exaggerated aescin-induced apoptosis

TIGAR regulates autophagy and apoptosis in response to starvation and ROS [8]. Aescin elevates the levels of cellular ROS [26], which are key upstream signals to activate autophagy [27]. Next, we investigated the role of TIGAR in regulating autophagy and apoptosis in response to aescin. The results showed that aescin apparently increased the level of LC3-II with treatment of 20, 40, and 80 μg/mL aescin for 12 h or treatment of 40 μg/mL aescin for 6, 9, 12, and 24 h in HCT-116 cells (Fig. 6a, b), which indicated that aescin-activated autophagy. To determine the increase of autophagosome biogenesis or the decrease of autophagosome clearance in response to aescin, Bafilomycin A1 (Baf. A1), an inhibitor of autophagosome-lysosome fusion, was used to impede autophagosome clearance. As shown in Fig. 6c, Baf. A1 increased the levels of LC3-II and p62 in HCT-116 cells. Of

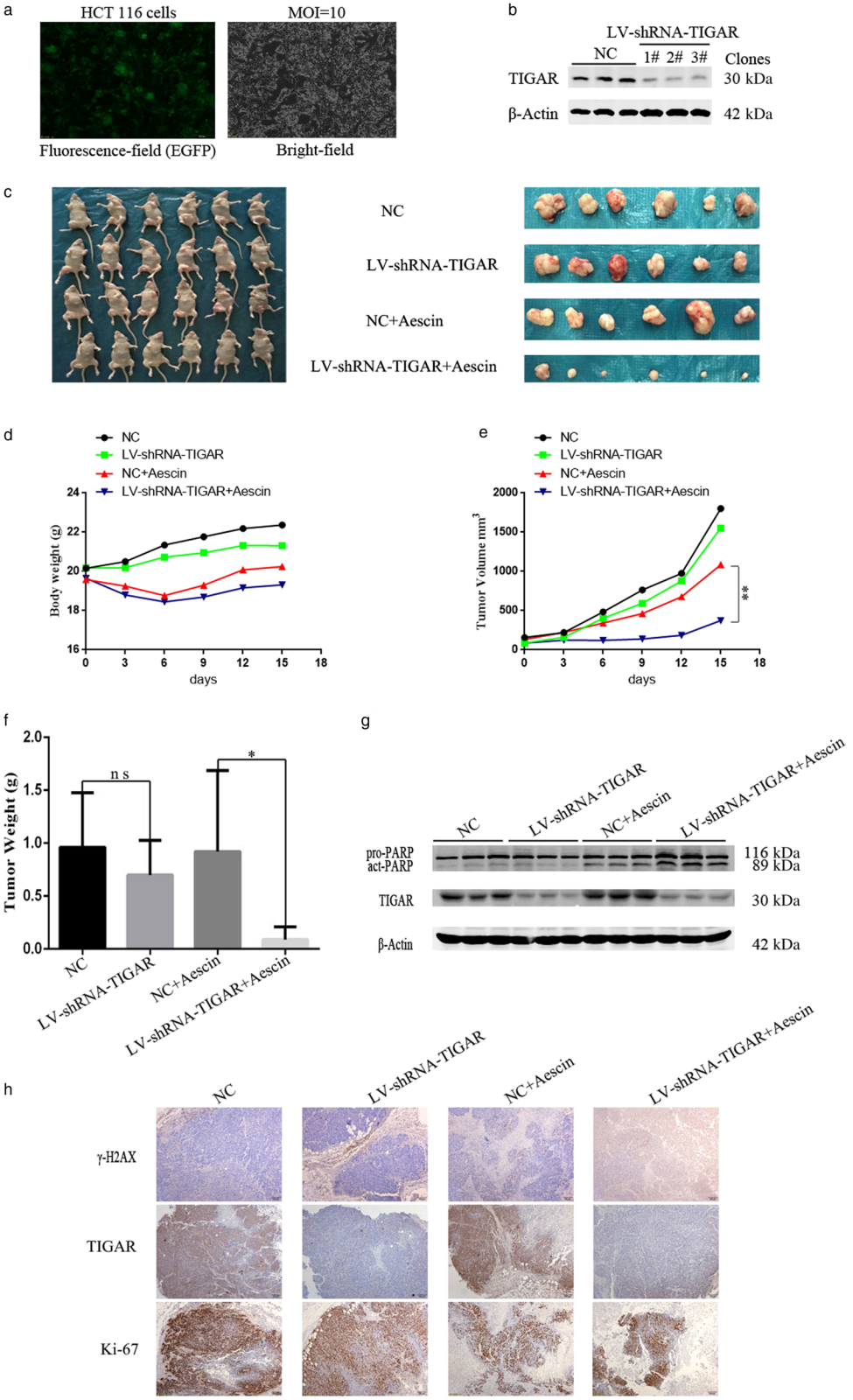

Fig. 5 Knockdown of TIGAR enhanced the anticancer effect of aescin in vivo. **a** The infection efficiency analysis of HCT-116 cells by fluorescence microscopy. Cells were infected with vector or EGFP-LV-shRNA-TIGAR (MOI = 10). **b** The levels of TIGAR and β-actin in NC and three clones by WB. Three clones (1#, 2#, and 3#) were selected in medium with 4 μg/mL puromycin for 2 weeks. **c** The mice ($n = 6$) with different sizes of tumors in right iliac fossa and the tumors that were dissected from various groups of mice. **d** The body weight of mice in various groups. **e** The comparison of tumor volumes in various groups. **f** Quantitative analysis of the tumor weight in various groups. **g** The levels of PRAP, TIGAR, and β-actin in tumor tissues of various groups by WB. **h** Immunohistochemistry analysis of the levels of γ-H2AX, TIGAR, and Ki-67 in various groups of tumor tissues. β-actin was used as a loading control. $^{*}P < 0.05$; $^{**}P < 0.01$; $^{ns}P > 0.05$ vs. corresponding group

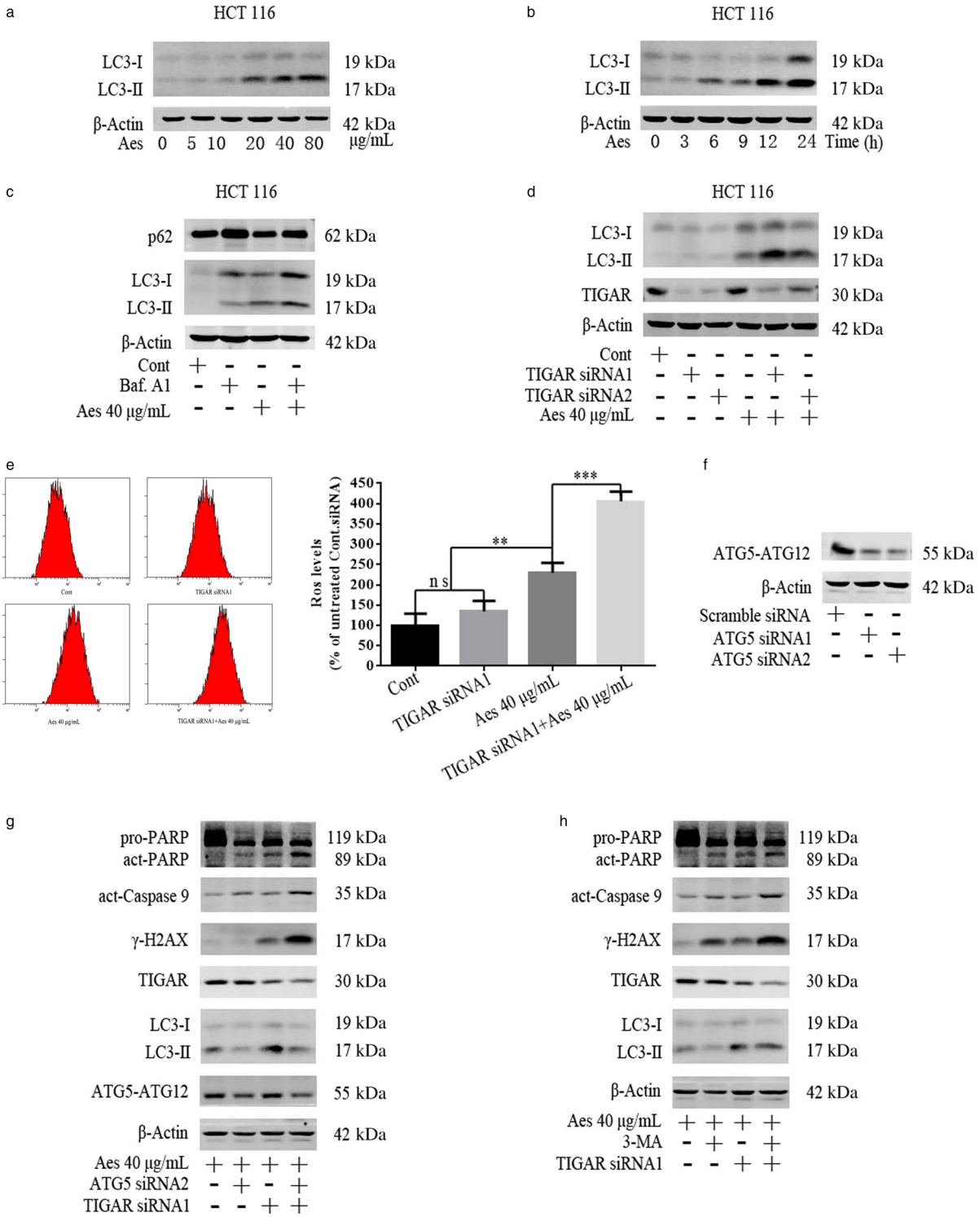

Fig. 6 Aescin-activated autophagy and inhibition of autophagy and TIGAR exaggerated aescin-induced apoptosis. **a**, **b** The levels of LC3-I, LC3-II, and β-actin in HCT-116 cells by WB. Cells were treated with 0, 5, 10, 20, 40, and 80 μg/mL aescin for 12 h or treated with 40 μg/mL aescin for 0, 3, 6, 9, 12, and 24 h. **c** The levels of LC3-I, LC3-II, p62, and β-actin in HCT-116 cells by WB. Cells were treated with/without 100 nM Bafilomycin A1 (Baf. A1) and/or 40 μg/mL aescin for 12 h. **d** The levels of LC3-I, LC3-II, TIGAR, and β-actin in HCT-116 cells by WB. Cells were treated with or without 40 μg/mL aescin for 12 h after cells were transfected with *TIGAR* siRNA1 or *TIGAR* siRNA2 for 36 h. **e** FCM analysis of ROS in HCT-116 cells. Cells were treated with or without 40 μg/mL aescin for 12 h after cells were transfected with *TIGAR* siRNA1 for 36 h. **f** The levels of ATG5-ATG12 and β-actin in HCT-116 cells by WB. Cells were transfected with Scramble siRNA, *ATG5* siRNA1, or *ATG5* siRNA2 for 48 h. **g**, **h** The levels of PRAP, activated caspase-9, γ-H2AX, TIGAR, LC3-I, LC3-II, ATG5-ATG12, and β-actin in HCT-116 cells by WB. Cells were treated with 40 μg/mL aescin for 12 h after cells were transfected with *TIGAR* siRNA1 and/or *ATG5* siRNA2 for 36 h (**g**). Cells were transfected with *TIGAR* siRNA1 for 36 h, then pretreated with 3-MA for 12 h before cells were treated with 40 μg/mL aescin for 12 h (**h**). β-actin was used as a loading control. The values are means ± SD from three independent experiments. $^{**}P < 0.01$, $^{***}P < 0.001$, $^{ns}P > 0.05$ vs. control group

note, the elevated level of LC3-II induced by aescin was further increased in the presence of Baf.A1, suggesting that aescin induced apparent augmentation of autophagosome formation rather than reduced autophagosome clearance.

Our previous study shows that knockdown of TIGAR activates epirubicin-induced autophagy, which exerts a pro-survival function in cancer cells [15]. We next investigated whether knockdown of TIGAR further activates aescin-induced autophagy. As we speculated, knockdown of TIGAR further increased the level of LC3-II induced by aescin (Fig. 6d), suggesting that inhibition of TIGAR elevated aescin-induced autophagy. ROS serve as the upstream signaling pathway in activating autophagy in many models. Consistent with previous studies, aescin increased the levels of ROS, which were further elevated by TIGAR knockdown in HCT-116 cells.

We next investigated the role of autophagy in response to aescin when TIGAR was knocked down. Autophagy inhibition was performed with *ATG5* siRNAs or 3-MA, which is an inhibitor of class I PI3K and class III PtdIns3K, and suppresses the class III PtdIns3K to inhibit autophagy [32]. As shown in Fig. 6f, the level of ATG5-ATG12 was markedly decreased when *ATG5* siRNA1 and *ATG5* siRNA2 were transiently transfected into HCT-116 cells. Furthermore, inhibition of autophagy or TIGAR knockdown using siRNAs mildly increased the levels of activated PARP and activated caspase-9 in aescin-treated HCT-116 cells (Fig. 6g). More importantly, inhibition of autophagy and TIGAR knockdown significantly increased the levels of activated PARP, activated caspase-9, and γ-H2AX, indicating that inhibition of autophagy and TIGAR synergistically augmented aescin-induced apoptosis (Fig. 6g). Similarly, 3-MA or *TIGAR* siRNA1 mildly increased the levels of activated PARP, activated caspase-9, and γ-H2AX (Fig. 6h). Moreover, 3-MA and *TIGAR* siRNA1 apparently increased the levels of these proteins (Fig. 6h). These results demonstrated that TIGAR knockdown further enhanced aescin-induced ROS and autophagy. Inhibition of the elevated autophagy exaggerated aescin-induced apoptosis.

DISCUSSION

Aescin exerts anticancer effects and increases cellular ROS [26]. In this study, we found that TIGAR played important roles in aescin's anticancer effects via regulating autophagy and apoptosis. Aescin not only induced DNA damage and autophagy activation, but also upregulated TIGAR protein levels. Knockdown of TIGAR exacerbated aescin-induced DNA damage, apoptosis, and autophagy activation. Knockdown of TIGAR and/or inhibition of autophagy enhanced aescin's anticancer effects in vitro or in vivo. Thus, TIGAR plays protective roles in cancer cells by inhibiting DNA damage and apoptosis, but TIGAR limited autophagy activity and this action is unfavorable to cancer cell survival.

TIGAR is overexpressed in various types of cancer tissues. TIGAR, as a stress response protein, is upregulated in different kinds of stress, including starvation [8], hypoxia [33], ionizing radiation [34], DNA damage, and chemotherapeutic drug treatment [15]. In addition, TIGAR regulates cancer cell metabolism to confer cell survival in mild stress. TIGAR lowers ROS and autophagy to reduce apoptosis in response to starvation and hypoxia via metabolism conversion from glycolysis to PPP. Following the DNA damage reaction, apoptosis, a prominent route response to the lesion, is induced and various signal pathways are involved in the reaction [35]. Moreover, many chemical genotoxins induce apoptosis because of the consequence of retarding the DNA replication [30]. Thus, severe DNA damage may lead to cell apoptosis and TIGAR may regulate cancer cell apoptosis via modulating ROS, autophagy, and DNA damage and repair.

In the present study, we found that aescin upregulated the expression of TIGAR in cancer cells (Fig. 3). Considering the carcinogenic functions of TIGAR in CRC tissue [13] and intestinal adenoma model [14], we strived to demonstrate the functions of TIGAR in aescin's anticancer effects. Consistent with the previous studies, TIGAR exerted positive functions to antagonize the anticancer effects of aescin, as our results showed that TIGAR knockdown aggravated aescin-induced DNA damage and apoptosis (Fig. 3), and also enhanced aescin's anticancer effects in vivo, indicating the protective functions of TIGAR on cancer cells (Fig. 5). On the contrary, overexpression of TIGAR reduced aescin-induced DNA damage and apoptosis (Fig. 4). Notably, replenishment of NADPH and ribose partly rescued the DNA damage and apoptosis induced by aescin and TIGAR knockdown (Fig. 4). These results suggest that TIGAR plays key protective roles in response to aescin via metabolic regulation and its downstream products of NADPH and ribose.

Autophagy is stimulated by multiple forms of stress, such as metabolic stress, endoplasmic reticulum (ER) stress, hypoxia, DNA damage, and elevated ROS [36]. Autophagy is one of defense mechanisms against oxidative stress damage [37]. Furthermore, there is a crosstalk between autophagy and apoptosis, and the activation of autophagy and the context determine the roles of autophagy in cancer [38]. Although we have illustrated the dual functions of TIGAR in modulating autophagy and apoptosis in HCC cells [15], the complexity of autophagy in various cancers or in the same cancer at the different stages may play positive or negative functions in affecting the progress and the chemo-sensitivity of cancers, which makes us to further explore whether the dual regulatory effects of TIGAR on cancer cells also occur in other cancers or in response to other chemo-drugs. In response to aescin-induced stress and damage reaction, autophagy, as a defensive action, was activated by aescin (Fig. 6). Concurrently, TIGAR, as a stress response protein, was also upregulated by aescin. There were two protective reactions in response to aescin, one is the increase of TIGAR protein levels, and the other is the increase in autophagy activity. Does TIGAR play dual functions in aescin-treated cancer cells via regulating autophagy and apoptosis? Our results showed that knockdown of TIGAR increased aescin-induced autophagy and ROS (Fig. 6). The elevated autophagy protected cancer cells, as inhibition of autophagy exacerbated the DNA damage and apoptosis induced by aescin and TIGAR knockdown (Fig. 6). Collectively, these results underline a protective role of autophagy in the anticancer effects of aescin, indicating TIGAR has a dual role in determining cancer cell fate via inhibiting both apoptosis and autophagy in response to aescin in CRC cells.

The mechanisms of TIGAR in modulating autophagy and apoptosis in vivo may be complicated in various context. The functions of TIGAR in vivo may be different from in vitro. To further demonstrate the functions of TIGAR in promoting cancer progress in vivo, we inhibited the expression of TIGAR using lentivirus. Consistent with the in vitro results, inhibition of TIGAR enhanced the anticancer effects of aescin in vivo, suggesting that TIGAR may be a therapeutic target in treatment of CRC [14]. In addition, we also found the decrease of body weight when aescin was administrated in the first week, suggesting some toxic effects with treatment of aescin in vivo. Moreover, aescin exhibited the toxic effects in normal colon NCM460 cells (Fig. 1c), which may limit the clinical application in treatment of CRC. However, in combination with TIGAR knockdown, or autophagy suppression may provide strategies to reduce the dose of aescin and the side effects, while increases the anticancer efficacy.

In conclusion, TIGAR was upregulated in response to aescin and played key roles in aescin-induced apoptosis via regulating DNA damage and repair, ROS, and autophagy. Hence, targeting the regulation of TIGAR expression or autophagy could represent a promising therapeutic strategy for enhancement of the anticancer effects of aescin in CRC therapeutic interventions.

ACKNOWLEDGEMENTS

This work was supported by grants from National Natural Science Foundation of China (No. 81770483 and 81602613), Jiangsu Provincial Commission of Health and Family Planning (No. YG201402 and YG201503), Jiangsu Provincial Medical Youth Talent (No. QNRC2016249), Jiangsu Provincial Science and Technology office (No. BL2014043), Suzhou Science and Technology Bureau (No. SYSD2013041, SYSD2016044, SYSD2017041, and SYS201788), Suzhou Health and Family Planning Commission Program (No. LCZX201504), Wujiang District Science and Technology Bureau (No. WS201301), and Wujiang District Commission of Health and Family Planning (No. WWK201607 and WWK201609).

AUTHOR CONTRIBUTIONS

All listed authors contributed to the idea generation, design, and completion of this study. B.L., Z.W., and J.-M.X. contributed equally to the idea generation, experimental work, and manuscript preparation; G.W., L.-Q.Q., X.-M.G., and X.-P.S. contributed to the experimental work and manuscript preparation; X.-Q.L., Q.-G.G., G.-H.S., and Z.-H. Q. guided the idea generation, experimental work, and manuscript preparation. All authors reviewed the manuscript.

ADDITIONAL INFORMATION

Competing interests: The authors declare no competing interests.

REFERENCES

1. Brenner H, Kloor M, Pox CP. Colorectal cancer. Lancet. 2014;383:1490–1502.
2. Siegel RL, Miller KD, Jemal A. Cancer statistics, 2017. CA Cancer J Clin. 2017;67:7–30.
3. Siegel RL, Miller KD, Fedewa SA, Ahnen DJ, Meester RGS, Barzi A, et al. Colorectal cancer statistics, 2017. CA Cancer J Clin. 2017;67:177–93.
4. Holohan C, Van Schaeybroeck S, Longley DB, Johnston PG. Cancer drug resistance: an evolving paradigm. Nat Rev Cancer. 2013;13:714–26.
5. Fearon ER. Molecular genetics of colorectal cancer. Annu Rev Pathol. 2011;6:479–507.
6. Markowitz SD, Bertagnolli MM. Molecular origins of cancer: molecular basis of colorectal cancer. N Engl J Med. 2009;361:2449–60.
7. Bensaad K, Tsuruta A, Selak MA, Vidal MN, Nakano K, Bartrons R, et al. TIGAR, a p53-inducible regulator ofglycolysis and apoptosis. Cell. 2006;126:107–20.
8. Bensaad K, Cheung EC, Vousden KH. Modulation of intracellular ROS levels by TIGAR controls autophagy. EMBO J. 2009;28:3015–26.
9. Won KY, Lim SJ, Kim GY, Kim YW, Han SA, Song JY, et al. Regulatory role ofp53 in cancer metabolism via SCO2 and TIGAR in human breast cancer. Hum Pathol. 2012;43:221–8.
10. Wanka C, Steinbach JP, Rieger J. Tp53-induced glycolysis and apoptosis regulator (TIGAR) protects glioma cells from starvation-induced cell death by up- regulating respiration and improving cellular redox homeostasis. J Biol Chem. 2012;287:33436–46.
11. Qian S, Li J, Hong M, Zhu Y, Zhao H, Xie Y, et al. TIGAR cooperated with glycolysis to inhibit the apoptosis of leukemia cells and associated with poor prognosis in patients with cytogeneti-cally normal acute myeloid leukemia. J Hematol Oncol. 2016;9:128.
12. Wong EY, Wong SC, Chan CM, Lam EK, Ho LY, Lau CP, et al. TP53-induced glycolysis and apoptosis regulator promotes proliferation and invasiveness of nasopharyngeal carcinoma cells. Oncol Lett. 2015;9:569–74.
13. Al-Khayal K, Abdulla M, Al-Obeed O, Al Kattan W, Zubaidi A, Vaali-Mohammed MA, et al. Identification of the TP53-induced glycolysis and apoptosis regulator in various stages of colorectal cancer patients. Oncol Rep. 2016;35:1281–6.
14. Cheung EC, Athineos D, Lee P, Ridgway RA, Lambie W, Nixon C, et al. TIGAR is required for efficient intestinal regeneration and tumorigenesis. Dev Cell. 2013;25:463–77.
15. Xie JM, Li B, Yu HP, Gao QG, Li W, Wu HR, et al. TIGAR has a dual role in cancer cell survival through regulating apoptosis and autophagy. Cancer Res. 2014;74:5127–38.
16. Yu HP, Xie JM, Li B, Sun YH, Gao QG, Ding ZH, et al. TIGAR regulates DNA damage and repair through pentosepho-sphate pathway and Cdk5-ATM pathway. Sci Rep. 2015;5:9853.
17. Patlolla JM, Raju J, Swamy MV, Rao CV. Beta-escin inhibits colonic aberrant crypt foci formation in rats and regulates the cell cycle growthbyinducingp21(waf1/cip1) in colon cancer cells. Mol Cancer Ther. 2006;5:1459–66.
18. Tan SM, Li F, Rajendran P, Kumar AP, Hui KM, Sethi G. Identification of beta-escin as a novel inhibitor of signal transducer and activator oftranscription 3/Janus-activated kinase 2 signaling pathway that suppresses proliferation and induces apoptosis in human hepatocellular carcinoma cells. J Pharmacol Exp Ther. 2010;334:285–93.
19. Ji DB, Xu B, Liu JT, Ran FX, Cui J. R. beta-Escin sodium inhibits inducible nitric oxide synthase expression via downregulation of the JAK/STAT pathway in A549 cells. Mol Carcinog. 2011;50:945–60.
20. Harikumar KB, Sung B, Pandey MK, Guha S, Krishnan S, Aggarwal BB. Escin, a pentacyclic triterpene, chemosensitizes human tumor cells through inhibition of nuclear factor-kappaB signaling pathway. Mol Pharmacol. 2010;77:818–27.
21. Ming ZJ, Hu Y, Qiu YH, Cao L, Zhang XG. Synergistic effects of beta-aescin and 5-fluorouracil in human hepatocellular carcinoma SMMC-7721 cells. Phytomedicine. 2010;17:575–80.
22. Wang YW, Wang SJ, Zhou YN, Pan SH, Sun B. Escin augments the efficacy of gemcitabine through down-regulation of nuclear factor-kappaB and nuclear factor-kappaB-regulated gene products in pancreatic cancer both in vitro and in vivo. J Cancer Res Clin Oncol. 2012;138:785–97.
23. Huang GL, Shen DY, Cai CF, Zhang QY, Ren HY, Chen QX. Beta-escin reverses multidrug resistance through inhibition of the GSK3beta/beta-catenin pathway in cholangiocarcinoma. World J Gastroenterol. 2015;21:1148–57.
24. Lee HS, Hong JE, Kim EJ, Kim SH. Escin suppresses migration and invasion involving the alteration of CXCL16/CXCR6 axis in human gastric adenocarcinoma AGS cells. Nutr Cancer. 2014;66:938–45.
25. Wang Y, Xu X, Zhao P, Tong B, Wei Z, Dai Y. Escin Ia suppresses the metastasis of triple-negative breast cancer by inhibiting epithelial-mesenchymal transition via down-regulating LOXL2 expression. Oncotarget. 2016;7:23684–99.
26. Mojzisova G, Kello M, Pilatova M, Tomeckova V, Vaskova J, Vasko L, et al. Anti-proliferative effect of beta-escin - an in vitro study. Acta Biochim Pol. 2016;63:79–87.
27. Kroemer G, Marino G, Levine B. Autophagy and the integrated stress response. Mol Cell. 2010;40:280–93.
28. Fang LM, Li B, Guan JJ, Xu HD, Shen GH, Gao QG, et al. Transcription factor EB is involved in autophagy-mediated chemoresistance to doxorubicin in human cancer cells. Acta Pharmacol Sin. 2017;38:1305–16.
29. Qian L, Liu Y, Xu Y, Ji W, Wu Q, Liu Y, et al. Matrine derivative WM130 inhibits hepatocellular carcinoma by suppressing EGFR/ERK/MMP-2 and PTEN/AKT signaling pathways. Cancer Lett. 2015;368:126–34.
30. Roos WP, Kaina B. DNA damage-induced cell death by apoptosis. Trends Mol Med. 2006;12:440–50.
31. Lee P, Hock AK, Vousden KH, Cheung EC. p53- and p73-independent activation of TIGAR expression in vivo. Cell Death Dis. 2015;6:e1842.
32. Seglen PO, Gordon PB. 3-Methyladenine: specific inhibitor of autophagic/ lysosomal protein degradation in isolated rat hepatocytes. Proc Natl Acad Sci U S A. 1982;79:1889–92.
33. Cheung EC, Ludwig RL, Vousden KH. Mitochondrial localization of TIGAR under hypoxia stimulates HK2 and lowers ROS and cell death. Proc Natl Acad Sci U S A. 2012;109:20491–6.
34. Zhang H, Gu C, Yu J, Wang Z, Yuan X, Yang L, et al. Radiosensitization of glioma cells by TP53-induced glycolysis and apoptosis regulator knockdown is dependent on thioredoxin-1 nuclear translocation. Free Radic Biol Med. 2014;69:239–48.
35. Jackson SP, Bartek J. The DNA-damage response in human biology and disease. Nature. 2009;461:1071–8.
36. Mizushima N, Komatsu M. Autophagy: renovation of cells and tissues. Cell. 2011;147:728–41.
37. Zhang L, Wang K, Lei Y, Li Q, Nice EC, Huang C. Redox signaling: potential arbitrator of autophagy and apoptosis in therapeutic response. Free Radic Biol Med. 2015;89:452–65.
38. White E. Deconvoluting the context-dependent role for autophagy in cancer. Nat Rev Cancer. 2012;12:401–10.